Fluorescence Lifetime and Spectral Characteristics of Subretinal Drusenoid Deposits and Their Predictive Value for Progression of Age-Related Macular Degeneration

Sebastian Weber,[1] Rowena Simon,[1] Linda-Sophia Schwanengel,[1] Christine A. Curcio,[2] Regine Augsten,[1] Daniel Meller,[1] and Martin Hammer[1,3]

[1]Department of Ophthalmology, University Hospital Jena, Jena, Germany
[2]Department of Ophthalmology and Visual Sciences, School of Medicine, University of Alabama at Birmingham, Birmingham, Alabama, United States
[3]Center for Medical Optics and Photonics, Univ. of Jena, Jena, Germany

Correspondence: Martin Hammer, University Hospital Jena, Department of Ophthalmology, Am Klinikum 1, 07747 Jena, Germany; martin.hammer@med.uni-jena.de.

Received: September 21, 2022
Accepted: December 3, 2022
Published: December 29, 2022

Citation: Weber S, Simon R, Schwanengel LS, et al. Fluorescence lifetime and spectral characteristics of subretinal drusenoid deposits and their predictive value for progression of age-related macular degeneration. *Invest Ophthalmol Vis Sci.* 2022;63(13):23. https://doi.org/10.1167/iovs.63.13.23

Purpose. To measure fundus autofluorescence (FAF) lifetimes and peak emission wavelengths (PEW) of subretinal drusenoid deposits (SDD) in age-related macular degeneration (AMD) and their development over time.

Methods. Fluorescence lifetime imaging ophthalmoscopy (FLIO) was performed in 30 eyes with optical coherence tomography (OCT)–confirmed early or intermediate AMD and SDD. Contrasts of mean lifetimes in short- (SSC) and long-wavelength channels (LSC), PEW, and relative fluorescence intensity were determined as differences of the respective measures at individual SDD and their environment. Measurements were made at baseline and at follow-up intervals 1 (13–36 months) and 2 (37–72 months), respectively.

Results. Of 423 SDD found at baseline, 259, 47, and 117 were hypoautofluorescent, isoautofluorescent, and hyperautofluorescent, respectively. FAF lifetimes of SDD were significantly longer than those of their environment by 14.5 ps (SSC, 95% confidence interval [CI], 13.3–15.7 ps) and 3.9 ps (LSC, 3.1-4.7 ps). PEW was shorter by 1.53 nm (1.07–1.98 nm, all contrasts $P < 0.001$) with higher contrasts for hyperfluorescent SDD. Over follow-up, SDD tended to hyperautofluorescence (relative intensities increased by 3.4% [95% CI, 2.9%–4.1%; $P < 0.001$] in follow-up 2). Hyperautofluorescence was associated with disruption of the ellipsoid zone on OCT. Disease progression to late-stage AMD was associated with higher lifetime contrast in SSC (15.9ps [14.2–17.6 ps] vs. 11.7 ps [9.9–13.5 ps], $P < 0.001$) at baseline.

Conclusions. SDD show longer FAF lifetimes and shorter PEW than their environments. A high lifetime contrast of SDD in SSC might predict disease progression to late-stage AMD.

Keywords: age-related macular degeneration, subretinal drusenoid deposits, fundus autofluorescence, fluorescence lifetime, fluorescence spectra, retinal pigment epithelium

Age-related macular degeneration (AMD) is a globally prevalent disease of aging that is managed medically in the 15% of patients with exudative complications and lacks a targeted treatment for the remaining 85%. Initial trial results for inhibitors of complement cascade proteins, the largest risk factor implicated by genetics, show promise in slowing the expansion of atrophy.[1,2] Treatments at earlier stages of disease, before irreversible tissue and visual damage, remains a research priority, motivating a search for prognostic biomarkers in clinical imaging.

A model of pathophysiology to emerge from 15 years of treating exudative AMD as guided by structural optical coherence tomography (OCT) is the concept of deposit-driven end stages.[3] In this model, two layers of extracellular deposits, on apical and basal aspects of retinal pigment epithelium (RPE), presage distinct forms of neovascularization and atrophy.[4] Remarkably these deposits mirror the topography of cone and rod photoreceptors, thus linking clinical appearance to the evolutionary and developmental biology of the fovea. Soft druse material clusters under the cone-rich fovea[5,6] and leads directly to neovascularization of choroidal origin. Subretinal drusenoid deposits (SDD, also called *reticular pseudodrusen*) first appear near the superior vascular arcades where rods are abundant and indicate risk for neovascularization of retinal origin, at sites closer to the fovea than the deposits themselves.[7] Differential deposit lipid composition has led to the proposal that SDD and drusen represent dysregulated transfers among the cells supporting rod- and cone-specific physiology. Depending on the patient population and imaging technology, 30% to-40% of eyes with intermediate AMD may have SDD, which constitute an independent risk factor for progression.[8–10]

SDD are dynamic and undergo growth and regression.[11] Macular SDD have a dot or ribbon appearance on color

Table 1. Patient Demographics, AMD Progression, and SDD Count

	Baseline	Follow-Up 1 (13–36 mo)	Follow-Up 2 (37–72 mo)
N (patients)	26 (100%)	16 (62%)	9 (35%)
Female	15 (58%)	8 (50%)	5 (56%)
Male	11 (42%)	8 (50%)	4 (44%)
Age (years, mean ± SD)	75.2 ± 7.7	75.6 ± 7.8	76.3 ± 8.9
N (eyes)	30 (100%)	19 (63%)	11 (37%)
Eyes progressed to MNV	5 (17%)		
Eyes progressed to cRORA/GA	5 (17%)		
SDD			
Total	423 (100%)	257 (61%)	124 (29%)
Hypofluorescent	259 (61%)	160 (62%)	45 (36%)
Isofluorescent	47 (11%)	28 (11%)	26 (21%)
Hyperfluorescent	117 (28%)	69 (27%)	53 (43%)

AMD progression was determined irrespective of the time point of appearance for all patients (i.e. also for subjects who had no follow-up FLIO). It is given in the column "baseline" to make clear that the numbers and percentages refer to all eyes included at baseline.

fundus photography (CFP) extend into the mid periphery.[12] SDD are classified by size and morphologic disturbance of neighboring photoreceptors into four stages: diffuse, mound-like, ellipsoid zone (EZ) disruption, and regression.[13] SDD are best identified and distinguished from sub-RPE drusen by OCT.[13] Near infrared (IR) imaging shows SDD as hyporeflective dots, and when EZ is disrupted, a central hyper-reflectivity surrounded by a hyporeflective annulus is seen.[14] By CFP,[15] SDD are slightly bluer than sub-RPE drusen. In short-wavelength fundus autofluorescence (FAF) imaging,[14] most SDD appear hypoautofluorescent. So far, one study also reported hyperautofluorescent SDD.[16]

Fluorescence lifetime imaging ophthalmoscopy (FLIO) is a laser-scanning based technique to further characterize FAF by measuring the time a molecule remains in an excited state before returning to the ground state upon emission of a fluorescence photon.[17,18] FLIO revealed lengthening of FAF lifetimes in cross-sectional[19] and longitudinal studies[20] of patients with AMD. This might be related to pathologic changes in the RPE, because a lengthening of FAF lifetimes, along with a hypsochromic shift of the emission spectrum, was found in activated, anteriorly migrated RPE cells.[21] Whereas the FAF lifetimes of soft drusen may or may not differ from their environment,[19,22] lengthening of lifetimes in SDD is reported.[23] Furthermore, generally longer FAF lifetimes were seen in AMD patients having SDD compared to eyes with soft drusen and no SDD.[24]

In this study, we measured FAF lifetimes, as well as spectral characteristics of individual SDD in patients with early or intermediate AMD over follow-up times of up to 6 years. We explored the capability of these FAF parameters to predict the disease progression to late-stage AMD.

Methods

Subjects and Procedures

From an ongoing longitudinal study in 68 eyes with early and intermediate AMD undergoing FLIO, we selected those patients having any SDD for this analysis. Patients with late-stage AMD (either geographic atrophy [GA] in CFP, complete RPE and outer retinal atrophy [cRORA] in OCT, or macular neovascularization [MNV][25]) at baseline were excluded. Further exclusion criteria were vascular occlusion, diabetic retinopathy, macular telangiectasia type 2, and hereditary retinal dystrophies. Also, patients with advanced cataract were excluded if the image quality in FLIO, as well as in OCT was insufficient to decide on the presence of SDD. Follow-up investigations were performed up to 72 months. For the quantitative analysis, results were grouped into two follow-up intervals: follow-up 1 (13–36 months, mean: 24.7 ± 6.7 months) and follow-up 2 (37–72 months, mean 53.2 ± 9.4 months). If a patient had more than one investigation within one follow-up interval, the latest investigation was used. Patient demographic data at baseline and follow-up visits are given in Table 1.

The study was approved by the ethics committee of the University Hospital Jena and adhered to the tenets of the Declaration of Helsinki. All participants gave written informed consent before study inclusion and underwent a full ophthalmologic examination including best corrected visual acuity, OCT (Cirrus-OCT 5000; Carl-Zeiss Meditec AG, Jena, Germany; macula cube: 512 A-scans per 128 B-scans, axial resolution: 5 µm, lateral resolution: 15 µm) and CFP (Visucam; Carl-Zeiss Meditec AG). Pupils were dilated using tropicamide (Mydriaticum Stulln; Pharma Stulln GmbH, Nabburg, Germany) and phenylephrine hydrochloride (Neosynephrin-POS 5%; Ursapharm GmbH, Saarbrucken, Germany). After pupil dilation, patients received FLIO imaging. No sodium fluorescein was administered to the cornea or by intravenous injection before the FLIO investigation.

Disease progression to late-stage AMD was determined as transition to cRORA[26] in OCT/GA in CFP or to macular neovascularization, determined by fluorescein angiography. Clinical follow-up investigation and AMD staging was done for all subjects included at baseline, irrespective of follow-up FLIO investigations, and describes incidence over a 72-month time course.

FLIO Imaging and Data Analysis

Basic principles and laser safety of FLIO are described elsewhere.[12,17,18] The recording of FLIO images is based on 473 nm picosecond laser diode excitation (repetition rate of 80 Mhz), coupled with a laser scanning ophthalmoscope (Spectralis, Heidelberg Engineering, Heidelberg, Germany). Fluorescence photons were detected by time-correlated single photon counting (SPC-150, Becker & Hickl GmbH, Berlin, Germany) in a short-wavelength (SSC: 498–560 nm) and a long-wavelength (LSC: 560–720 nm) spectral channel. FLIO provides 30° field images with a frame

Investigative Ophthalmology & Visual Science

rate of nine frames per second and a resolution of 256 × 256 pixels. Photon histograms over time per pixel, describing the autofluorescence decay, were least square fitted with a series of three exponential functions using the software SPCImage 6.0 (Becker & Hickl GmbH, Berlin, Germany). The amplitude-weighted mean decay time τ_m, called FAF lifetime, was used for further analysis. The resulting image is color-coded, depicting short lifetimes in red and long lifetimes in blue. In addition, the peak emission wavelength (PEW) of the fluorescence was determined from the ratio of photon counts (autofluorescence intensity) in SSC and LSC as described by Schultz et al.[27]

One grader (S.W.) manually segmented all SDD identified in OCT as regions of interest (ROI) in FAF images using the software FLIMX, which is documented and freely available for download under an open-source Berkeley Software Distribution license (http://www.flimx.de).[28] Mean FAF lifetimes and PEW per pixel were averaged over all pixels of the ROI, as well as the environment of the ROI, defined as a 105-µm–wide area, 35 µm distant to the ROI, and surrounding the ROI. In case of confluent or near-confluent SDD, pixels nearer than 35 µm to another SDD were omitted from the environment (Supplemental Fig. S1). Contrasts (i.e., differences between lifetimes or PEW, respectively) at the SDD and their environments were calculated for each deposit and used for further analysis. The relative FAF intensity of the SDD was determined as a ratio of photon counts, averaged over the pixels of each SDD and its environment. This way, we distinguished hypoautofluorescent (ratio < 0.975), isoautofluorescent (0.975≤ ratio ≤1.025) and hyperautofluorescent SDD (ratio > 1.025).

Statistics

SPSS 27.0 (IBM, SPSS Inc., Chicago, IL, USA) was used for statistical analysis. A mixed linear model was fitted for the outcome parameters lifetimes, PEW, and relative fluorescence intensity to account for correlated data since multiple SDD per eye were analyzed and both eyes were included in four subjects. Depending on the aim of the analysis, group or timepoint (baseline, follow-up 1, follow-up 2) are modelled as fixed effects. Post hoc pairwise comparisons used Bonferroni correction to compensate for multiple testing. The significance level was set at 0.05.

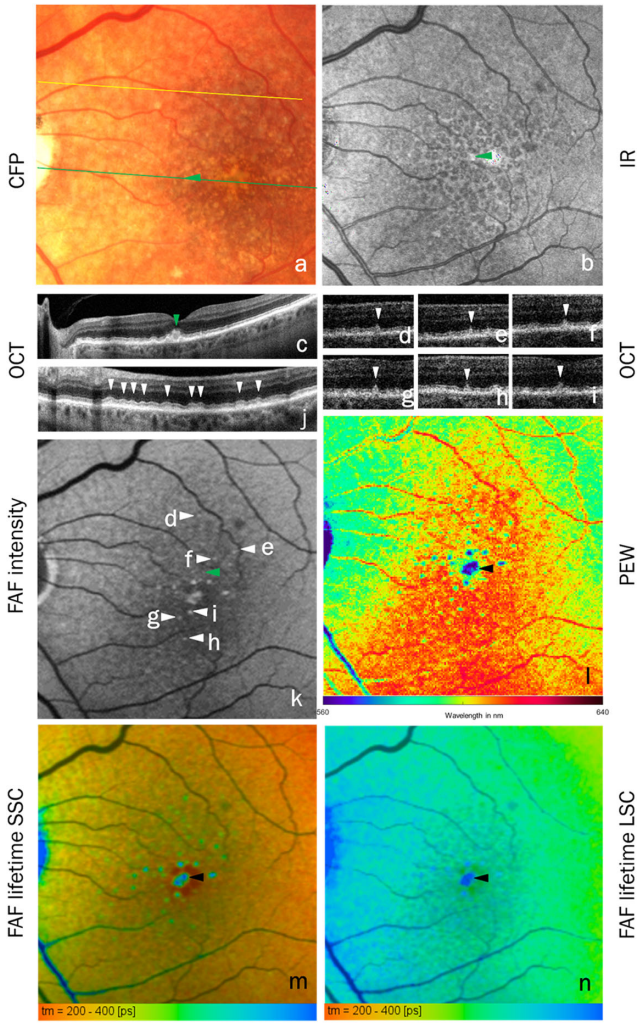

Figure 1. Eighty-five-year old male patient with SDD and AVL (green arrowheads): CFP **(a)**, IR **(b)**, OCT **(c)** at *green line* in **a**, OCT **(j)** at *yellow line* in **a** ,SDD annotated with *white arrowheads* in **(d–j)**, FAF **(k)**, PEW **(l)**, FLIO SSC **(m)**, and FLIO LSC **(n)**. Although most SDD are hypofluorescent, some (panels **d–i** and respective *arrowheads* in **k**) are hyperfluorescent and penetrate the ellipsoid zone (panels **d–i**). Hypo-fluorescent SDD show an intact ellipsoid zone (**panel j,** *arrowheads*).

Results

FLIO signals associated with 423 SDD in 30 eyes of 26 patients were investigated at baseline. Between three and 33 SDD per eye were analyzed (mean 13.9 ± 8-9). All but two eyes (93.4%) had soft drusen as well.

A typical example is shown in Figure 1. Two-hundred-fifty-nine out of 423 OCT-confirmed SDD were hypoautofluorescent relative to their environments, as expected from previous literature, yet still have measurable autofluorescence. Furthermore, by careful investigation we found 47 isoautofluorescent and 117 hyperautofluorescent SDD as well (Table 1).[16,29] Hyperautofluorescence was associated with the disruption of the EZ: 28 of the 30 SDD with highest relative intensity were stage 3 according to Zweifel et al.[13] (i.e., showing EZ disruption). An acquired vitelliform lesion (AVL) was seen in four eyes. Nine of the 30 SDD with highest relative FAF intensities were seen in eyes that also had AVL.

The FAF lifetimes of SDD were significantly longer than that of their environment by 14.5 ps (SSC: 95% CI, 13.3–15.7 ps) and 3.9 ps (LSC: 95% CI, 3.1–4.7 ps). SDD PEW was shorter than that of their environments by 1.53 nm (95% CI, 1.07–1.98 nm, all contrasts $P < 0.001$). A subgroup analysis (Table 2) showed that lifetime and PEW contrasts differed significantly among hypoautofluorescent (N = 259, 61.2%), isoautofluorescent (N = 47 [11.1%]), and hyperautofluorescent (N = 117 [27.7%]) SDD ($P < 0.001$ for all measures); lifetimes lengthened (i.e., contrasts increased) from hypoautofluorescent to hyperautofluorescent SDD, whereas PEW shortened. All group comparisons were highly significant (Table 2). Considering all SDD, the contrasts of PEW were negatively correlated, and those of lifetimes were positively correlated with the intensity ratio ($P < 0.001$ for all, Fig. 2). In other words, brighter SDD in FAF had longer lifetimes and shorter emission wavelength.

Table 2. Contrasts of Fluorescence Lifetimes and PEW Of Hypofluorescent, Isofluorescent, and Hyperfluorescent SDD

	N	Hypofluorescent Mean (95% CI)	Isofluorescent Mean (95% CI)	Hyperfluorescent Mean (95% CI)
Contrast PEW SSD - vicinity				
Hypofluorescent	259	–0.12 (–0.66 to 0.37) nm	$P < 0.001$	$P < 0.001$
Isofluorescent	47		–3.70 (–4.82 to –2.58) nm	$P < 0.001$
Hyperfluorescent	117			–9.33 (–10.22 to –8.45) nm
Contrast τ_m SSC SSD – vicinity				
Hypofluorescent	259	11.35 (10.00 to 12.71) ps	$P = 0.007$	$P < 0.001$
Isofluorescent	47		18.10 (13.97 to 22.23) ps	$P = 0.002$
Hyperfluorescent	117			27.10 (24.21 to 29.99) ps
Contrast τ_m LSC SSD - vicinity				
Hypofluorescent	259	0.94 (–1.32 to 3.20) ps	$P < 0.001$	$P < 0.001$
Isofluorescent	47		5.12 (3.09–7.16) ps	$P < 0.001$
Hyperfluorescent	117			13.00 (11.49–114.57) ps

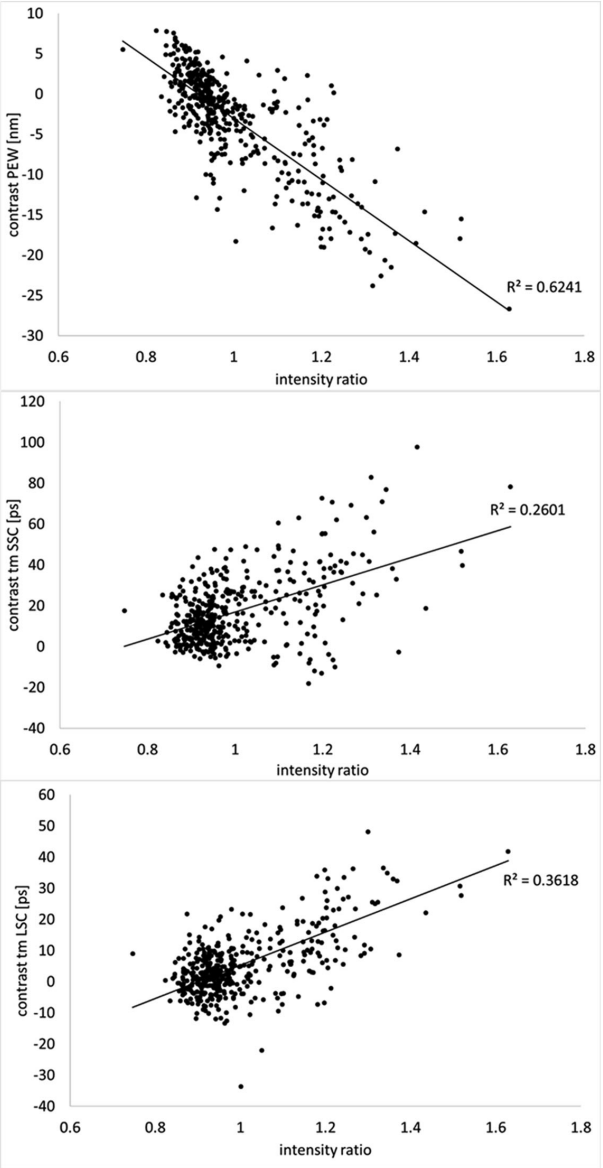

Figure 2. Peak emission wavelength (PEW, *top*), FAF lifetime SSC (*middle*), and LSC (*bottom*) versus fluorescence intensity ratio of SDD and environment. The 95% confidence intervals of the correlation coefficients R^2 are 0.564–0.677 (PEW), 0.190–0.333 (τ_m SSC), and 0.328–0.434 (τ_m LSC), all $P < 0.001$.

For hypoautofluorescent SDD, the contrast of lifetimes differed significantly from zero. However, this difference was relevant in SSC (10.7 ps; 95% CI, 9.6–11.82 ps; $P < 0.001$) but only 1.06 ps (95% CI, 0.48–1.62 ps; $P = 0.002$) in LSC. Among these deposits, PEW did not differ significantly. Isoautofluorescent and hyperautofluorescent SDD showed significant contrasts for lifetimes and PEW (all $P \leq 0.004$). The contrasts of hyperautofluorescent SDD were remarkable in both SSC-lifetime (25.3 ps; 95% CI, 21.7–28.7 ps) and PEW (−9.2 nm; 95% CI, −10.7 to −7.7 nm).

Two-hundred-fifty-seven SDD were found in 19 eyes at follow-up 1 (13–36 months). At follow-up 2 (37-72 months) we found 124 SDD in 11 eyes (Table 3). Whereas there was no change in the fraction of hypoautofluorescent, isoautofluorescent, and hyperautofluorescent SDD from baseline to follow-up 1, the fraction of hypoautofluorescent SDD decreased, and that of hyperautofluorescent SDD increased in follow-up 2 (Table 1). In total, the SDD got brighter (i.e., the FAF intensity ratio increased from baseline by 3.4% [95% CI, 2.9%–4.1%; $P < 0.001$]) in follow-up 2 (no significance at follow-up 1). The FAF lifetime and PEW did not change over the follow-up (Table 3). The change of lifetimes and PEW versus follow-up time is given in supplemental Figure 2.

Seven hypoautofluorescent stage 3 SDD at baseline became hyperautofluorescent at follow-up 2. At baseline these SDD had longer lifetimes in SSCs than hypoautofluorescent SDD on average (contrast 22.8 ± 11.4 ps vs. 11.5 ± 10.3 ps; no significance test was performed because N = 7).

In one patient (Fig. 3), 26 out of 32 SDD regressed over a follow-up of 71 months. This eye developed a central GA on CFP, also seen as cRORA in OCT, associated with intraretinal fluid. However, all but one of the regressing SDD were outside the area developing atrophy in the follow-up. Also, no outer retinal atrophy (without RPE atrophy) was seen in this eye. All but one SDD that regressed at follow-up were hypoautofluorescent at baseline.

Compared to all other hypoautofluorescent SDD, regressing SDD had longer lifetimes (contrasts SSC 16.9 ps [95% CI, 13.5–20.3 ps] vs. 10.1 ps [95% CI, 8.9–11.2 ps], LSC: 5.2 ps [95% CI, 3.2–7.3 ps] vs. 0.5 ps [95% CI, −0.1 to 1.2 ps]; both $P < 0.001$); no difference in PEW was found. Ten of the 26 regressing SDD were in the scan area of the baseline OCT and were confirmed as stage 3. At follow-up, one regressing SDD was associated with a hyper-reflective focus on OCT. The other nine were unremarkable. After

Investigative Ophthalmology & Visual Science

Table 3. Contrasts of Fluorescence Lifetimes and PEW at Baseline and Follow-Up 1 (13–26 Months) and Follow-Up 2 (37–72 Months)

	Baseline (N = 423)	Follow-up 1 (N = 257)	Follow-up 2 (N = 124)
Contrast PEW SSD – vicinity, (nm)	−1.80 (95% CI, −2.28 to −1.33)	−1.92 (95% CI, −2.57 to −1.27)	−2.60 (95% CI, −3.51 to −1.69)
Contrast τ_m SSC SSD – vicinity (ps)	15.1 (95% CI, 13.8–16.4)	9.8 (95% CI, 7.9–11.6)	11.4 (95% CI, 8.9–13.9)
Contrast τ_m LSC SSD – vicinity (ps)	3.7 (95% CI, 2.9–4.6)	0.7 (95% CI, -0.4–1.8)	4.2 (95% CI, 2.5–5.8)

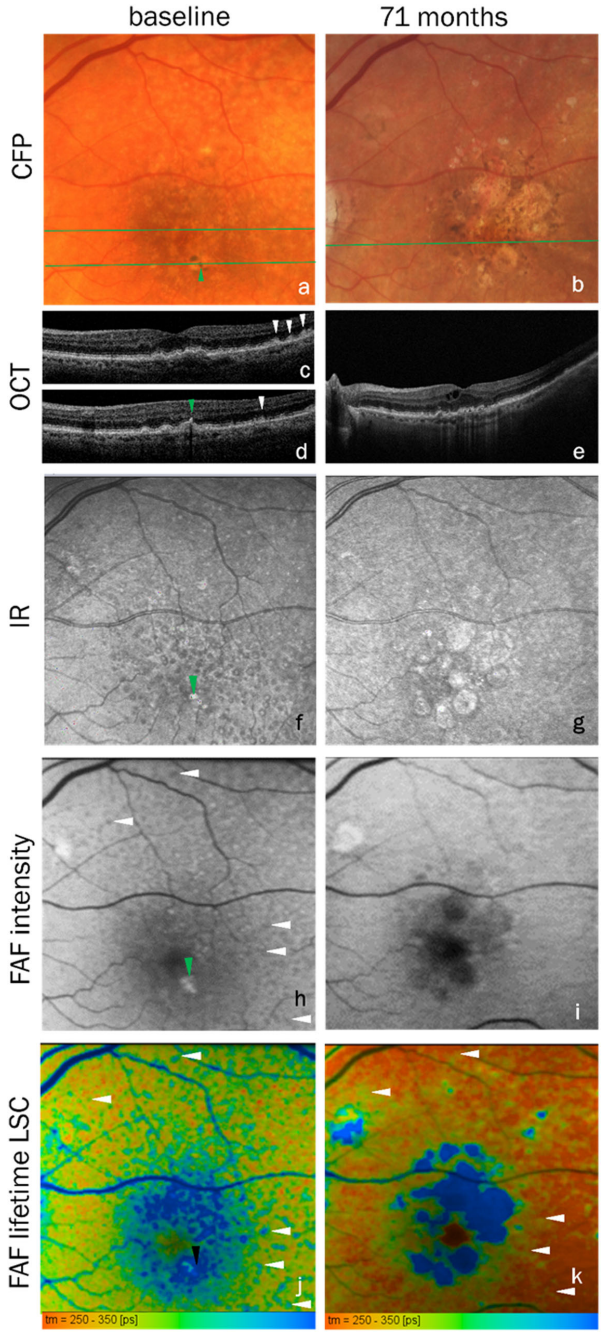

Figure 3. Eighty-year old female patient at baseline (*left*) and 71 months later (*right*): CFP **(a, b)**, OCT at green lines in **a** and **b (c–e)**, IR **(f, g)**, FAF **(h,i)**, and FLIO LSC **(j, k)**. The *white arrowheads* point to SDD at baseline, which regressed at follow-up, leaving spots of lifetimes longer than their environment (see panel **k**). The *green arrowhead* (*black* in panel **j**) points to a druse with RPE detaching from Bruch's membrane and migrating towards the retina. It shows hyperpigmentation **(a)** and hyperreflection in OCT **(d)** and leads to atrophy in follow-up.

regression of some SDD (white arrowheads in Fig. 3), lifetimes in SSC remained long. Others were unremarkable in FLIO at the follow-up. For comparison, a nonprogressing patient is shown in Supplemental Figure S3. SDD were growing in number and visibility in IR and FAF over the follow-up of 47 months.

One-third (10 out of 30) of the eyes progressed to either cRORA (n = 5) or to MNV (n = 5). For one patient no follow-up investigation was available. In SSC, SDD in patients with progression to late-stage AMD (N = 183) had longer lifetimes at baseline than SDD in nonprogressing patients (N = 228) (contrasts 15.9 ps [95% CI, 14.2–17.6 ps] vs. 11.7 ps [95% CI, 9.9–13.5 ps], $P < 0.001$). This holds for patients progressing to MNV (18.5 ps [95% CI, 15.3–21.7 ps] vs. 12.8 ps [95% CI, 11.5–14.1 ps], $P = 0.005$) and not for progression to cRORA. LSC lifetime and PEW did not differ between progressing and non-progressing eyes. The patients with and without AMD progression did not differ significantly in age (72.3 ± 8.9 vs. 6.7 ± 6.8 years; $P = 0.247$).

Thirty-five hyperautofluorescent SDD were found in 10 eyes progressing to advanced AMD (average 1.5 per eye), whereas 71 hyperautofluorescent SDDs were found in 12 nonprogressing eyes (3.55 per eye). The ratio of hyperautofluorescent to hypoautofluorescent SDD was 0.30 in progressing and 0.50 in nonprogressing eyes.

Discussion

As seen by others,[13,30] most of our SDD were hypoautofluorescent. However, isoautofluorescent[14] and hyperautofluorescent SDD were also found, supporting a finding from one group to date.[16,29]

Morphology of SDD in histology and their possible effects on FAF are illustrated in Figure 4. Hypoautofluorescence of SDD may result from the absorption of fluorescence light (excitation as well as emission) from the underlying RPE by SDD (Figs. 4B–D).[16] Although reduced disk shedding and phagocytosis could contribute to fewer bisretinoid fluorophores in RPE [31] (Fig. 4C), this possibility needs to be assessed with higher-resolution microscopy than available in the published literature. Finally, SDD can cause RPE to thin and thus reduce FAF.[8]

Hyperautofluorescence is associated with some stage 3 SDD and may have various causes. The extracellular deposit may be fluorescent itself. SDD contain unesterified cholesterol,[32] apolipoprotein E,[33] vitronectin,[34,35] CD59,[36] and in larger deposits, some photoreceptor outer segment disk membranes (Figs. 4D, 4E),[37,38] all of which are nonfluorescent upon irradiation with blue light in microscopy studies. Melanolipofuscin granules, showing green fluorescence (Fig. 4E), were illustrated in one published case with abundant SDD.[8] Melanolipofuscin has a slightly shorter fluorescence emission wavelength than lipofuscin[39] and could contribute to both a fluorescent signal and a hypsochromic shift if present in sufficient numbers. Reduced absorption of light by degenerated or deflected photoreceptor outer segments,[40] along with thinning of the outer nuclear layer,[35]

Investigative Ophthalmology & Visual Science

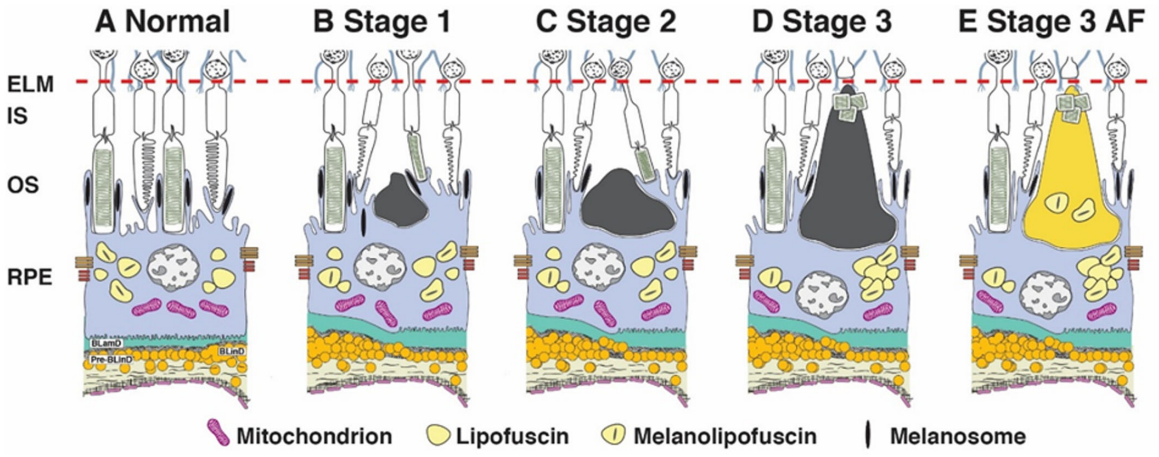

Figure 4. Hypothesized modulators of outer retinal autofluorescence signal associated with SDD. Schematic is adapted from Chen et al.[37] to demonstrate a model of anatomical and physical factors influencing fluorescence lifetimes. Drawing is not to scale. Stages 1-3 of Zweifel et al.[13] are shown as dark gray to represent lack of FAF signal. A Stage 3 AF has been added as one possible explanation for the increase of FAF associated with SDD over time. As elaborated in the text, appearance of net greater FAF could result from the appearance of new fluorophores in SDD, the decrease of existing absorbers in adjoining photoreceptors, increased RPE fluorescence, or a combination. ELM, external limiting membrane; IS, OS, inner and outer segment of photoreceptor, RPE, retinal pigment epithelium; BLamD, basal laminar deposit; pre-BLinD, pre-basal linear deposit. **(A)** Normal aged RPE has outer segments embedded in melanosome-containing apical processes and autofluorescent lipofuscin and melanolipofuscin in the cell body. **(B)** Aged RPE with small SDD thought to correspond to stage 1 of OCT is associated with shorter, deflected outer segments. **(C)** At Stage 2 of OCT, in which the EZ line is elevated, inner segments are now uneven in length, and some OS are deflected. **(D)** At Stage 3 of OCT, overlying photoreceptors retract their inner segments or die, leading to the loss of EZ visibility in OCT. Some large deposits have evidence of outer segment fragments with disks still visible.[37] **(E)** Signal in Stage 3 AF may result from new fluorophores appearing in SDD, depicted as a change in color.

might increase the incident light on RPE fluorophores and thus increase FAF intensity (Fig. 4E). Finally, RPE dysmorphia (rounding, stacking, anterior migration), also seen in AMD,[41] can cause hyperautofluorescence because of increased pathlength of light through cells with fluorophores.[21,22,42,43] Although we cannot exclude spectral filter effects by SDD or photopigments (or their absence) affecting apparent RPE fluorescence, these effects should alter spectra (PEW) but not lifetimes.

Our finding of longer FAF lifetimes associated with clinically visualized SDD agrees with longer lifetimes in the outer ETDRS ring in AMD patients, regardless of whether eyes had drusen or SDD, reported by Dysli et al.[23] These authors did not determine local contrasts as done here. We found longer lifetimes associated with SDD than their environments predominantly in SSC. As lipofuscin is known to emit predominantly at wavelengths above 560 nm, this suggests participation by non-lipofuscin fluorophores in SDD or adjacent anatomical structures. Even in hypoautofluorescent SDD, a minor contribution of those fluorophores might be indicated by the positive lifetime contrast. Their concentration seems to increase in hyperautofluorescent SDD, as suggested by a further lengthening of SDD lifetimes.

Currently we have limited knowledge about the nature of these fluorophores. Melanolipofuscin is a candidate (see above). A contribution of nicotinamide adenine dinucleotide, flavin adenine dinucleotide, and retinol fluorescence[44] is unlikely because these fluorophores localize to cells rather than extracellular material and excite using different conditions from those used for FLIO. Also, RPE remodeling (e.g., loss or gain of specific organelle types that alter fluorophore composition) may also alter fluorescence lifetime and spectra.[21] Because lifetime in SSC remained long after OCT-confirmed SDD regression (Fig. 3), an alteration of RPE fluorescence is likely. This corresponds with our recent observation of a reduced PEW and increased FAF lifetimes in pathologically activated RPE in vivo,[21] as well as in histology (Simon et al., submitted). Microscopy studies of RPE flat mounts revealed enlarged hyperautofluorescent cells in AMD,[45,46] some with hypsochromic spectral shift, even in normal eyes.[47]

Over time, SDD became more hyperautofluorescent, as shown by a greater intensity ratio and a shift in the balance of hyperautofluorescent and hypoautofluorescent lesions in follow-up 2. This could suggest an accumulation of fluorescent material. However, it also might indicate a distortion of the photoreceptor outer segments (Figs. 4B–E) resulting in reduced photopigment density[48] or decrease of their length.[4,33] On the other hand, another study found shorter outer segment lengths in eyes with regressing SDD only.[49] Generally, however, FAF intensity should be considered cautiously, as changes over time are small and highly variable over individual SDD. Furthermore, our data suggest that, despite a real or apparent increase of SDD fluorescence intensity, the relevant fluorophore composition does not change, as FAF lifetimes and PEW are stable over time.

We found that SDD are associated with drusen in 93.4% of the eyes. Thus SDD- and drusen-specific pathways to late-stage AMD[50,51] may be seen in the same eye. However, the hazard ratio for progression to late AMD was not independently increased by SDD in a larger sample of patients having large soft drusen as well.[52] On the other hand, Spaide et al.[53] found a significant risk of progression to late-stage AMD in eyes with SDD and lacking drusen, and Xu et al.[54] found RPE atrophy associated with SDD. Here, we investigated whether FAF lifetime, PEW, or intensity is associated with disease progression to late AMD. Hyperautofluorescent SDD have been described before.[16] They differ from hypoautofluorescent and isoautofluorescent SDD in lifetime, PEW, and

morphology: Stage 3 SDD may or may not be hyperautofluorescent, whereas hyperautofluorescent SDD all (but two) were stage 3. However, in agreement with Lee et al.,[16] we found hyperautofluorescent SDD were not predictors of AMD progression, because the ratio of hyperautofluorescent to hypoautofluorescent SDD was lower in progressing versus nonprogressing eyes. On the other hand, a longer lifetime in SSC might be predictive for progression to advanced AMD because lengthening was significant for all progressing eyes.

Of the 30 most hyperautofluorescent SDD, seen in the 30 study eyes, nine were found in the four eyes with AVL. An association of SDD and AVL was reported by Spaide et al.,[53] who stated that "diminutive vitelliform deposits" develop in eyes with SDD and become hyperautofluorescent. AVL is a pathway to advanced AMD but is not specific to AMD. It contains an extracellular deposit and liberated RPE granules.[55] A recent histologic analysis concluded that these granules could not account for the entirety of autofluorescent AVL material. However, limited data on small AVL,[56,57] which may not include a deposit, also indicate the presence of isolated fluorescent organelles released by degenerating RPE. As noted above these could contribute to AF signal from AVL.

A strength of the current study is the use of multimodal imaging, comprising CFP, OCT, FAF, and FLIO, providing lifetime, as well as PEW information, in a cohort of AMD patients followed-up over up to six years. A limitation is the small number of subjects because of drop-out from follow-up investigations and the variable intervals as dictated by clinical needs. This limits predictions of progression by lifetimes. Nevertheless, despite variable follow-up, longer lifetimes for the progressing eyes were found. Because we only included SDD seen in OCT, we possibly missed some small SDD and biased the sample toward larger SDD.

In conclusion, this study found that (i) a considerable fraction of SDD was hyperautofluorescent, and hyperautofluorescence was associated with disruption of the EZ, (ii) SDD show longer FAF lifetimes and shorter PEW than their environments, and these contrasts correlate with the FAF intensity, (iii) the FAF intensity of SDD increases over their life cycle[58] with no change of FAF lifetimes or PEW, and (iv) a high lifetime contrast of SDD in SSC might predict disease progression to late-stage AMD.

Acknowledgments

Supported by NIH grants R01EY027948 and R01EY029595 and research support from Heidelberg Engineering.

Disclosure: **S. Weber**, None; **R. Simon**, None; **L.-S. Schwanengel**, None; **C.A. Curcio**, Apellis (C), Astellas (C), Genentech (C); **R. Augsten**, None; **D. Meller**, None; **M. Hammer**, None

References

1. Jaffe GJ, Westby K, Csaky KG, et al. C5 inhibitor avacincaptad pegol for geographic atrophy due to age-related macular degeneration: a randomized pivotal phase 2/3 trial. *Ophthalmology*. 2021;128:576–586.
2. Liao DS, Grossi FV, El Mehdi D, et al. Complement C3 inhibitor Pegcetacoplan for geographic atrophy secondary to age-related macular degeneration: a randomized phase 2 trial. *Ophthalmology*. 2020;127:186–195.
3. Spaide RF. Improving the age-related macular degeneration construct: a new classification system. *Retina*. 2018;38:891–899.
4. Curcio CA, Messinger JD, Sloan KR, McGwin G, Medeiros NE, Spaide RF. Subretinal drusenoid deposits in non-neovascular age-related macular degeneration: morphology, prevalence, topography, and biogenesis model. *Retina*. 2013;33:265–276.
5. Wang JJ, Rochtchina E, Lee AJ, et al. Ten-year incidence and progression of age-related maculopathy: the blue Mountains Eye Study. *Ophthalmology*. 2007;114:92–98.
6. Pollreisz A, Reiter GS, Bogunovic H, et al. Topographic distribution and progression of soft drusen volume in age-related macular degeneration implicate neurobiology of fovea. *Invest Ophthalmol Vis Sci*. 2021;62:26.
7. Haj Najeeb B, Deak G, Schmidt-Erfurth U, Gerendas BS. The Rap Study, Report Two: the regional distribution of macular neovascularization type 3, a novel insight into its etiology. *Retina*. 2020;40:2255–2262.
8. Wu Z, Fletcher EL, Kumar H, Greferath U, Guymer RH. Reticular pseudodrusen: a critical phenotype in age-related macular degeneration. *Prog Retin Eye Res*. 2021;88:101017.
9. Owsley C, Swain TA, McGwin G, et al. How Vision is impaired from aging to early and intermediate age-related macular degeneration: insights from ALSTAR2 baseline. *Transl Vis Sci Technol*. 2022;11:17.
10. Nassisi M, Lei J, Abdelfattah NS, et al. OCT risk factors for development of late age-related macular degeneration in the fellow eyes of patients enrolled in the HARBOR study. *Ophthalmology*. 2019;126:1667–1674.
11. Zhang Y, Wang X, Godara P, et al. Dynamism of dot subretinal drusenoid deposits in age-related macular degeneration demonstrated with adaptive optics imaging. *Retina*. 2018;38:29–38.
12. Suzuki M, Sato T, Spaide RF. Pseudodrusen subtypes as delineated by multimodal imaging of the fundus. *Am J Ophthalmol*. 2014;157:1005–1012.
13. Zweifel SA, Spaide RF, Curcio CA, Malek G, Imamura Y. Reticular pseudodrusen are subretinal drusenoid deposits. *Ophthalmology*. 2010;117:303–312.e301.
14. Querques G, Querques L, Martinelli D, et al. Pathologic insights from integrated imaging of reticular pseudodrusen in age-related macular degeneration. *Retina*. 2011;31:518–526.
15. Spaide RF, Curcio CA. Drusen characterization with multimodal imaging. *Retina-J Ret Vit Dis*. 2010;30:1441–1454.
16. Lee MY, Ham DI. Subretinal drusenoid deposits with increased autofluorescence in eyes with reticular pseudodrusen. *Retina*. 2014;34:69–76.
17. Schweitzer D, Schenke S, Hammer M, et al. Towards metabolic mapping of the human retina. *Microsc Res Tech*. 2007;70:410–419.
18. Dysli C, Quellec G, Abegg M, et al. Quantitative analysis of fluorescence lifetime measurements of the macula using the fluorescence lifetime imaging ophthalmoscope in healthy subjects. *Invest Ophthalmol Vis Sci*. 2014;55:2106–2113.
19. Sauer L, Gensure RH, Andersen KM, et al. Patterns of fundus autofluorescence lifetimes in eyes of individuals with nonexudative age-related macular degeneration. *Invest Ophthalmol Vis Sci*. 2018;59:AMD65–AMD77.
20. Schultz R, Hasan S, Schwanengel LS, Hammer M. Fluorescence lifetimes increase over time in age-related macular degeneration. *Acta Ophthalmol*. 2021;99:e970–e972.
21. Hammer M, Jakob-Girbig J, Schwanengel L, et al. Progressive dysmorphia of retinal pigment epithelium in age-related macular degeneration investigated by fluorescence lifetime imaging. *Invest Ophthalmol Vis Sci*. 2021;62:2.
22. Hammer M, Schultz R, Hasan S, et al. Fundus autofluorescence lifetimes and spectral features of soft drusen and hyperpigmentation in age-related macular degeneration. *Transl Vis Sci Technol*. 2020;9:20.

23. Dysli C, Fink R, Wolf S, Zinkernagel MS. Fluorescence lifetimes of drusen in age-related macular degeneration. *Invest Ophthalmol Vis Sci*. 2017;58:4856–4862.
24. Simon R, Curcio CA, Weber S, Meller D, Hammer M. Fluorescence lifetime and peak emission wavelength differ between AMD patients with soft drusen and sub-retinal drusenoid deposits. *Acta Ophthalmol*. 2022;100(6):e1354–e1355.
25. Spaide RF, Jaffe GJ, Sarraf D, et al. Consensus nomenclature for reporting neovascular age-related macular degeneration data: consensus on Neovascular Age-Related Macular Degeneration Nomenclature Study Group. *Ophthalmology*. 2020;127:616–636.
26. Sadda SR, Guymer R, Holz FG, et al. Consensus definition for atrophy associated with age-related macular degeneration on OCT: classification of Atrophy Report 3. *Ophthalmology*. 2018;125:537–548.
27. Schultz R, Klemm M, Meller D, Hammer M. Spectral calibration of fluorescence lifetime imaging ophthalmoscopy. *Acta Ophthalmol*. 2022;100(2):e612–e613.
28. Klemm M, Schweitzer D, Peters S, Sauer L, Hammer M, Haueisen J. FLIMX: a software package to determine and analyze the fluorescence lifetime in time-resolved fluorescence data from the human eye. *PLoS One*. 2015;10:e0131640.
29. Yoon JM, Shin DH, Kong M, Ham DI. Age-related macular degeneration eyes presenting with cuticular drusen and reticular pseudodrusen. *Sci Rep*. 2022;12:5681.
30. Lois N, Owens SL, Coco R, Hopkins J, Fitzke FW, Bird AC. Fundus autofluorescence in patients with age-related macular degeneration and high risk of visual loss. *Am J Ophthalmol*. 2002;133:341–349.
31. Spaide RF, Ooto S, Curcio CA. Subretinal drusenoid deposits AKA pseudodrusen. *Surv Ophthalmol*. 2018;63:782–815.
32. Curcio CA, Presley JB, Malek G, Medeiros NE, Avery DV, Kruth HS. Esterified and unesterified cholesterol in drusen and basal deposits of eyes with age-related maculopathy. *Exp Eye Res*. 2005;81:731–741.
33. Rudolf M, Malek G, Messinger JD, Clark ME, Wang L, Curcio CA. Sub-retinal drusenoid deposits in human retina: organization and composition. *Exp Eye Res*. 2008;87:402–408.
34. Hageman GS, Mullins RF, Russell SR, Johnson LV, Anderson DH. Vitronectin is a constituent of ocular drusen and the vitronectin gene is expressed in human retinal pigmented epithelial cells. *FASEB J*. 1999;13:477–484.
35. Greferath U, Guymer RH, Vessey KA, Brassington K, Fletcher EL. Correlation of histologic features with in vivo imaging of reticular pseudodrusen. *Ophthalmology*. 2016;123:1320–1331.
36. Ebrahimi KB, Fijalkowski N, Cano M, Handa JT. Decreased membrane complement regulators in the retinal pigmented epithelium contributes to age-related macular degeneration. *J Pathol*. 2013;229:729–742.
37. Chen L, Messinger JD, Zhang Y, Spaide RF, Freund KB, Curcio CA. Subretinal drusenoid deposit in age-related macular degeneration: histologic insights into initiation, progression to atrophy, and imaging. *Retina*. 2020;40:618–631.
38. Chen L, Messinger JD, Kar D, Duncan JL, Curcio CA. Biometrics, impact, and significance of basal linear deposit and subretinal drusenoid deposit in age-related macular degeneration. *Invest Ophthalmol Vis Sci*. 2021;62:33.
39. Warburton S, Davis WE, Southwick K, et al. Proteomic and phototoxic characterization of melanolipofuscin: correlation to disease and model for its origin. *Mol Vis*. 2007;13:318–329.
40. Zhang Y, Wang X, Rivero EB, et al. Photoreceptor perturbation around subretinal drusenoid deposits as revealed by adaptive optics scanning laser ophthalmoscopy. *Am J Ophthalmol*. 2014;158:584–596.e581.
41. von der Emde L, Vaisband M, Hasenauer J, et al. Histologic cell shape descriptors for the retinal pigment epithelium in age-related macular degeneration: a comparison to unaffected eyes. *Transl Vis Sci Technol*. 2022;11:19.
42. Ach T, Huisingh C, McGwin G, et al. Quantitative autofluorescence and cell density maps of the human retinal pigment epithelium. *Invest Ophthalmol Vis Sci*. 2014;55:4832–4841.
43. Rudolf M, Vogt SD, Curcio CA, et al. Histologic basis of variations in retinal pigment epithelium autofluorescence in eyes with geographic atrophy. *Ophthalmology*. 2013;120:821–828.
44. Berezin MY, Achilefu S. Fluorescence lifetime measurements and biological imaging. *Chem Rev*. 2010;110:2641–2684.
45. Ach T, Tolstik E, Messinger JD, Zarubina AV, Heintzmann R, Curcio CA. Lipofuscin redistribution and loss accompanied by cytoskeletal stress in retinal pigment epithelium of eyes with age-related macular degeneration. *Invest Ophthalmol Vis Sci*. 2015;56:3242–3252.
46. Zhang Q, Chrenek MA, Bhatia S, et al. Comparison of histologic findings in age-related macular degeneration with RPE flatmount images. *Mol Vis*. 2019;25:70–78.
47. Han M, Giese G, Schmitz-Valckenberg S, et al. Age-related structural abnormalities in the human retina-choroid complex revealed by two-photon excited autofluorescence imaging. *J Biomed Opt*. 2007;12:024012.
48. Mrejen S, Sato T, Curcio CA, Spaide RF. Assessing the cone photoreceptor mosaic in eyes with pseudodrusen and soft Drusen in vivo using adaptive optics imaging. *Ophthalmology*. 2014;121:545–551.
49. Spaide RF. Outer retinal atrophy after regression of subretinal drusenoid deposits as a newly recognized form of late age-related macular degeneration. *Retina*. 2013;33:1800–1808.
50. Smith RT, Sohrab MA, Busuioc M, Barile G. Reticular macular disease. *Am J Ophthalmol*. 2009;148:733–743.e732.
51. Xu L, Blonska AM, Pumariega NM, et al. Reticular macular disease is associated with multilobular geographic atrophy in age-related macular degeneration. *Retina*. 2013;33:1850–1862.
52. Wu Z, Kumar H, Hodgson LAB, Guymer RH. Reticular pseudodrusen on the risk of progression in intermediate age-related macular degeneration. *Am J Ophthalmol*. 2022;239:202–211.
53. Spaide RF, Yannuzzi L, Freund KB, Mullins R, Stone E. Eyes with subretinal drusenoid deposits and no drusen: progression of macular findings. *Retina*. 2019;39:12–26.
54. Xu X, Liu X, Wang X, et al. Retinal pigment epithelium degeneration associated with subretinal drusenoid deposits in age-related macular degeneration. *Am J Ophthalmol*. 2017;175:87–98.
55. Brinkmann M, Bacci T, Kar D, et al. Histology and clinical lifecycle of acquired vitelliform lesion, a pathway to advanced age-related macular degeneration. *Am J Ophthalmol*. 2022;240:99–114.
56. Chen KC, Jung JJ, Curcio CA, et al. Intraretinal hyperreflective foci in acquired vitelliform lesions of the macula: clinical and histologic study. *Am J Ophthalmol*. 2016;164:89–98.
57. Balaratnasingam C, Messinger JD, Sloan KR, Yannuzzi LA, Freund KB, Curcio CA. Histologic and optical coherence tomographic correlates in drusenoid pigment epithelium detachment in age-related macular degeneration. *Ophthalmology*. 2017;124:644–656.
58. Zhang Y, Wang X, Sadda SR, et al. Lifecycles of individual subretinal drusenoid deposits and evolution of outer retinal atrophy in age-related macular degeneration. *Ophthalmol Retina*. 2020;4:274–283.

Investigative Ophthalmology & Visual Science